JACS
JOURNAL OF THE AMERICAN CHEMICAL SOCIETY

Communication

pubs.acs.org/JACS

Light Makes a Surface Banana-Bond Split: Photodesorption of Molecular Hydrogen from $RuO_2(110)$

Michael A. Henderson,* Rentao Mu,† Arjun Dahal, Igor Lyubinetsky, Zdenek Dohnálek, Vassiliki-Alexandra Glezakou, and Roger Rousseau*

Physical Sciences Division, Physical & Computational Sciences Directorate, Pacific Northwest National Laboratory, Richland, Washington 99352, United States

Supporting Information

ABSTRACT: The coordination of H_2 to a metal center via polarization of its σ bond electron density, known as a Kubas complex, is the means by which H_2 chemisorbs at Ru^{4+} sites on the rutile $RuO_2(110)$ surface. This distortion of electron density off an interatomic axis is often described as a 'banana-bond.' We show that the Ru−H_2 banana-bond can be destabilized and split using visible light. Photodesorption of H_2 (or D_2) is evident by mass spectrometry and scanning tunneling microscopy. From time-dependent density functional theory, the key optical excitation splitting the Ru−H_2 complex involves an interband transition in RuO_2 which effectively diminishes its Lewis acidity, thereby weakening the Kubas complex. Such excitations are not expected to affect adsorbates on RuO_2 given its metallic properties. Therefore, this common thermal cocatalyst employed in photocatalysis is, itself, photoactive.

Model heterogeneous water splitting systems frequently incorporate supported cocatalyst functions specifically selected to promote redox reactions using charge carriers generated at light absorbing semiconductors.[1,2] Current understanding of the cooperative interactions between a photocatalyst and its supported cocatalyst is often limited to these narrowly defined roles. Yet just as semiconductor interfaces are not devoid of catalytic character, a cocatalyst should not be considered as photopassive. Here, we illustrate for the first time an inherent photochemical activity of RuO_2, a typical oxide material employed as a supported thermal cocatalyst in water splitting[3,4] and O_2 photoreduction[5] studies. We show that photon absorption in a thin (110)-oriented film of this rutile oxide grown on Ru(0001) results in photodesorption of molecular hydrogen.

Ruthenium oxide is well-known for its ability to catalyze oxidation reactions[6,7] and has received some attention for its potential in reductive chemistry.[8] This oxide has a long history in the photocatalytic literature for promoting thermal redox reactions, but has not been considered as a viable light absorber. The model rutile $RuO_2(110)$ surface has provided new fundamental insights into the role of RuO_2 in catalysis.[6] For example, Wang et al.[9] demonstrated that molecular hydrogen binds to the $RuO_2(110)$ surface at individual coordinatively unsaturated Ru^{4+} (Ru_{cus}) sites, desorbing thermally at ∼100 K. The adsorption structure[10] is believed to be Kubas-like,[11,12] in that the electron density of the H−H σ-bond is polarized toward the Ru_{cus} site, as is seen in many dihydrogen metal complexes.[13−15] The distorted electron density can be described as a banana-bond. Although the thermal dissociation for H_2 on $RuO_2(110)$ remains an open issue,[9,10,16−20] we illustrate in this work a new property of RuO_2, that of visible light activity splitting the Ru−H_2 σ-complex.

The adsorption/desorption properties of D_2 on $RuO_2(110)$ are examined using King and Wells sticking coefficient measurements[21] and temperature-programmed desorption (TPD). D_2 adsorbs on $RuO_2(110)$ at 40 K with an initial sticking probability of ∼0.4 (see the Supporting Information (SI)), yielding a desorption feature at 118 K (Figure 1A) which shifts to lower temperature with increased coverage, eventually peaking at 100 K for saturation. The trailing edges of a family of traces overlay suggestive of first-order desorption with a degree of coverage dependence. The D_2 TPD peak profile exhibits an asymmetry at 111 K for coverages above ∼0.5 ML, indicating a small change in the packing of D_2 molecules on the surface. Based on STM results (see below), the first layer saturation coverage of D_2 on the surface at 5−80 K is ∼0.75 ML, where 1 ML is designated as the Ru_{cus} site density on the ideal $RuO_2(110)$ surface (5.06×10^{14} cm^{-2}). The only other D_2 desorption feature detected is a broad, weak peak at ∼260 K (see Figure 2). The coverage in this peak is ∼3% of the saturation value, consistent with low defect densities on a well-defined $RuO_2(110)$ surface.

Aside from D_2 desorption, D_2O and HDO are also detected in TPD (see the SI), the latter arising from scrambling on the walls of the mass spectrometer and from small amounts of background H_2O adsorption. The surface chemistry responsible for water formation from hydrogen dissociation is detailed elsewhere[16,19,22,23] and therefore not a focus of this work. As shown in the SI, the upper limit on the amount of water generated from D_2 dissociation is ∼0.25 ML based on D_2O TPD.[24,25]

Using the inversion analysis approach,[26] Figure 1B displays the coverage-dependent binding energy (E_b) of D_2 on $RuO_2(110)$ obtained from the highest coverage TPD trace in Figure 1A. As expected, the E_b increases with decreasing coverage. Depending on selection of a prefactor, the E_b varies from 0.22 to 0.32 eV. In accord with the TPD assessment,

Received: May 17, 2016
Published: July 8, 2016

DOI: 10.1021/jacs.6b05083
J. Am. Chem. Soc. 2016, 138, 8714−8717

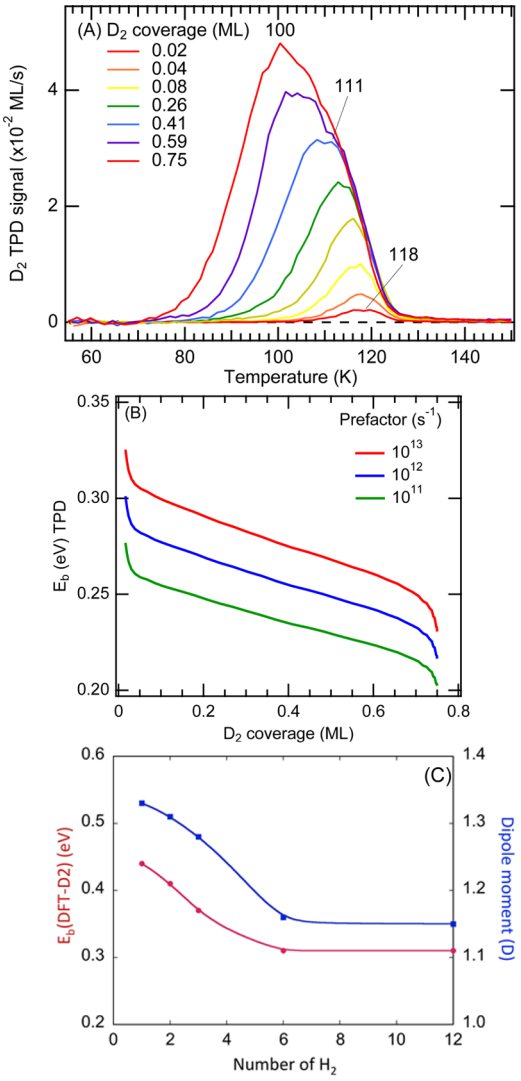

Figure 1. (A) D_2 TPD spectra (mass 4) from various coverages of D_2 on RuO_2(110) at 40 K. (B) The binding energy (E_b) obtained using the inversion method (see text) from the highest coverage TPD trace shown in 'A'. (C) DFT evaluation of E_b (red) for H_2 on RuO_2(110) as a function of coverage. The induced dipole on the H_2 molecule, μ, is plotted in blue.

DFT-D3 also shows that the ground-state E_b of H_2 at Ru_{cus} sites is dependent on the coverage, ranging from 0.31 to 0.44 eV (Figure 1C). The only bound configuration of H_2 at an Ru_{cus} site was the symmetric Kubas structure, though stable molecular and dissociative structures were found for adsorption at bridging O (O_b) sites, consistent with other theoretical studies.[10,19] Very little of the binding interaction at Ru_{cus} sites can be attributed to van der Waals dispersion forces, as our DFT-D3 estimate of this component was <0.1 eV. This observation, along with the repulsive nature of H_2−H_2 interactions on RuO_2(110), can be understood in terms of a simple electrostatic model.

Analysis based on maximally localized Wannier functions indicates that chemisorption primarily occurs by donation of the electron pair in the H−H bonding orbital to the $4d_{z^2}$ orbital of the strongly Lewis acidic Ru_{cus} site,[25] leading to a three-centered (3c)-2e$^-$ bonding interaction which is strongest at the low coverage extreme (1/12 ML), with the center of the Wannier function displaced by 0.15 Å off the bond center (as illustrated in Figure 3). This displacement is attenuated by 15% at higher coverages, effectively reducing the magnitude of the induced dipole from 1.33 D (at 1/12 ML) to 1.15 D (at 1 ML) (see Figure 1C and Table SI1). The induced dipoles were calculated as follows: a 2e$^-$ point charge is assigned to the center of the Wannier function at each H−H distance for different coverages (1/12, 1/6, 1/4, 1/2, and 1 ML). The resulting attenuation is indicative of parallel dipole−dipole interactions, separated by 3.1 Å at saturation, causing a depolarization of the Ru−H_2 interaction and a commensurate decrease in E_b (by ∼20%). A dipole image is consequently induced at the surface, estimated in a similar fashion by Wannier centers localized in the RuO_2 slab.

As a complementary point of analysis, inspection of the projected electronic density of states (pDOS) indicates that the H−H σ-bonding orbital becomes stabilized (by 5 eV) and broadened (by 0.8 eV), characteristic of a strong interaction with the continuum of Ru 4d states. Taken together, these results suggest that there is a significant electrostatic component to the Ru−H_2 bonding interaction, where the H_2 in the bound state is polarized by the Ru^{4+} center and also where the metallic nature of RuO_2 responds with a counter polarization within the oxide (as opposed to a well-defined sharp resonance associated with a localized bonding state).

Figure 2A presents TPD data illustrating the effect of visible light irradiation on D_2 adsorbed on RuO_2(110). For these data, an initial D_2 coverage of 0.70 ML is selected, and 460 nm light is employed. The data show that the 100 K TPD peak attenuates significantly with irradiation, and the broad 260 K feature is unchanged. Figure 2B shows the D_2 photon-stimulated desorption (PSD) trace, the only photodesorption channel detected, for the 4.4 × 10^{19} photon/cm^{-2} experiment shown in Figure 2A (the green trace). The near-exponential decay curve is consistent with first-order photodepletion of D_2 from the surface. The desorption event is distinctly nonthermal as the crystal temperature did not change and flux dependence shows the expected variation in rate. Coadsorption of a ∼1:1 mixture of H_2 and D_2 results in equivalent PSD contributions from these molecules without HD formation (see SI), indicating that photodesorption does not result from a recombinative process. The integrated PSD yield in Figure 2B corresponds to a coverage of ∼0.39 ML. The amounts of D_2 (Figure 2A) and water (see SI) in the subsequent TPD (i.e., after irradiation) decreased to 0.09 and 0.21 ML, respectively. This mass balance indicates an overall depletion of D_2 from surface as a result of light.

The ensemble-averaged TPD and PSD data are correlated in Figure 2C−E with atomic-scale observations using STM. The initial clean surface (Figure 2C) shows the expected bright and dark rows along the [001] direction of the RuO_2(110) surface associated with O_b and Ru_{cus} sites, respectively.[27] After saturation of the surface with H_2 at 5 K (Figure 2D), the image consists of superimposed bright linear arrays of adsorbed species on the Ru_{cus} rows. Irradiation of this H_2-saturated surface with broad band light (Hg arc lamp) results in depletion of H_2 molecules within the linear arrays, leaving behind a number of isolated species (Figure 2E). The overall H_2 coverage decreases from 0.75 ML (saturation) to ∼0.4 ML as a result of irradiation. These observations are consistent with the postirradiation TPD data that indicate depletion of H_2 (or D_2) from the surface.

As shown in Figure 3A, the Ru−H_2 bonding interaction can be modeled by a Morse potential, in this case using an H_2

DOI: 10.1021/jacs.6b05083
J. Am. Chem. Soc. 2016, 138, 8714−8717

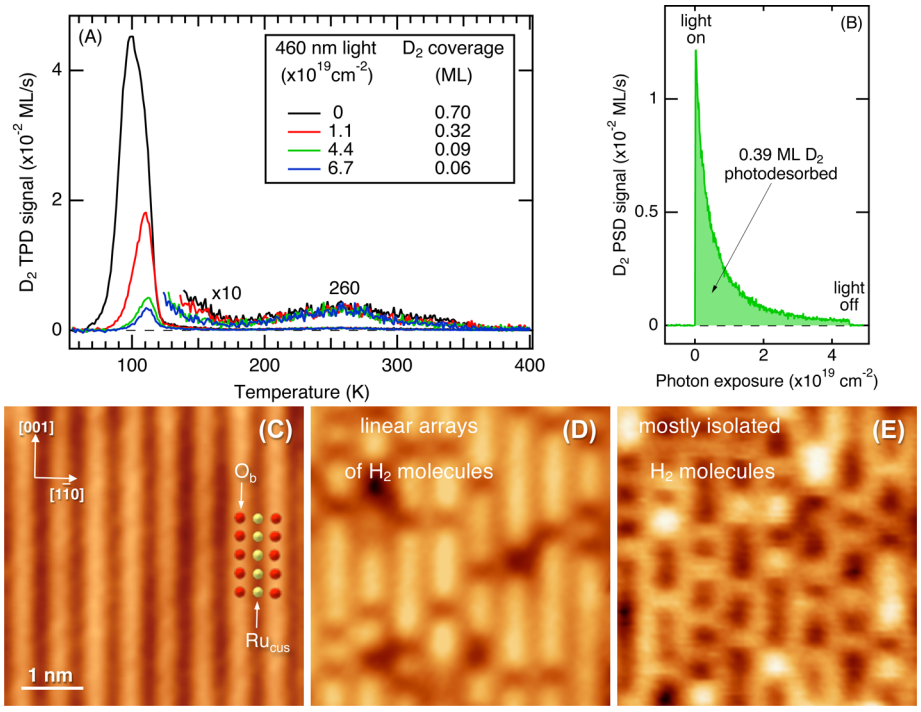

Figure 2. (A) TPD of D_2 (mass 4) after irradiation of 0.70 ML D_2 on RuO_2(110) at 40 K with various exposures of 460 nm light. (B) The D_2 PSD spectrum resulting from the 4.4×10^{19} cm^{-2} photon exposure in 'A'. (C–E) STM images of the clearn RuO_2(110) surface at 5 K before (C) and after (D) adsorption of 0.75 ML of H_2 and then following broad band irradiation for 90 min (E).

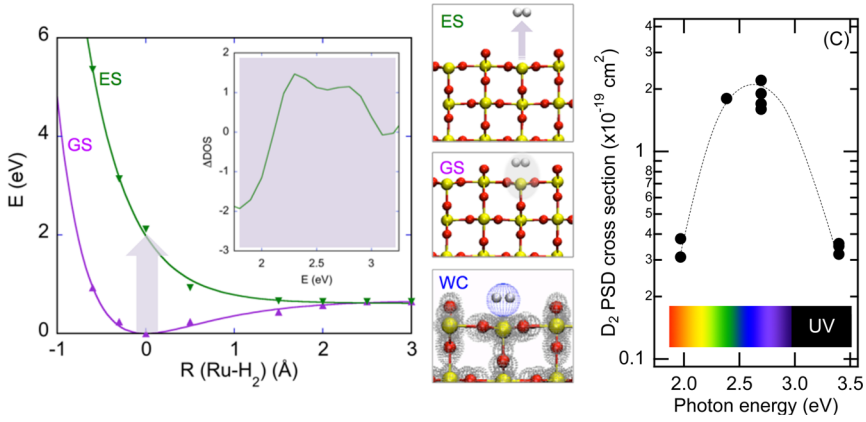

Figure 3. Ground (GS) and excited (ES) states for H_2 adsorption and photodesorption on RuO_2(110) (A) illustrate the electronic transition resulting in desorption (B). The inset in (A) shows the change in the spectral density of ESs between the adsorbed (positive) and desorbed (negative) configurations of the H_2/RuO_2 system, computed by TD-DFT calculations on a cluster; see details in text and SI. (B) Configurations corresponding to GS and ES from (A) as well as the location of the Wannier centers (WC, dotted spheres) used to depict the charge localization and polarization. Color scheme: H (white), O (red), Ru (yellow). (C) Log plot of the initial D_2 photodesorption rate from irradiation of 0.70 ML D_2 on RuO_2(110) at 40 K with four wavelengths of light: 630 (1.97 eV), 520 (2.38 eV), 460 (2.70 eV), and 365 nm (3.40 eV). Dashed curve is to guide the eye.

coverage of 1/12 ML (with E_b = 0.44 eV). The photodesorption process is addressed starting with this model of the ground state (GS) and consider two different approximations of the excited state (ES) electronic structure: (i) Using the charge constraint DFT formalism, we suppress the binding and polarization of the H_2 molecule by constraining the charge at the Ru_{cus} site and O atoms directly bound to it to resemble that of the clean surface. At 1/12 ML coverage, this constraint leads to a strictly repulsive potential described by an exponential function (Figure 3A), such that the GS-to-ES energy difference is on the order of 2.1 eV. (ii) The most definitive of analyses, however, comes from time-dependent DFT (TD-DFT) calculations of the ES energy manifold between 0 and 3.5 eV above E_F, as shown in the inset to Figure 3A (see SI). Using a cluster model where the local geometry, H_2-binding energy, and charge state at the Ru_{cus}–H_2 complex reproduce the surface slab calculations, we estimate the difference in the ES energy manifold with H_2 bound and unbound to the surface. H_2 adsorption induced a broad spectral change with a peak at ~2.5 eV, but only when H_2 was adsorbed. As experimental verification, Figure 3C shows that the D_2 PSD rate (i.e., photodepletion cross section) is greatest in the blue-green region of the visible spectrum (~2.5 eV).

DOI: 10.1021/jacs.6b05083
J. Am. Chem. Soc. 2016, 138, 8714–8717

Taken together, we attribute the photoinduced desorption of H_2/D_2 from $RuO_2(110)$ to be the result of depolarization of the induced dipole interaction within the Kubas complex resulting from an optical transition in the RuO_2 surface. This transition is most likely from O 2p derived states to unoccupied Ru 4d states based on the positions of p-to-d optically excited transitions in RuO_2.[28−30] Similar optical processes may occur on other late transition-metal oxides.[31]

The majority of photochemical events occurring at heterogeneous interfaces result from charge-transfer processes, i.e., the transfer of an electron between an interfacial state and an adsorbate resulting in bond-forming and/or bond-breaking events. Our findings suggest that H_2 photodesorption arises from a charge redistribution in the surface that weakens the electrostatics responsible for polarization of the H−H σ bond. Delving into time scales for these events—the initial electronic excitation, the stabilization of the charge redistribution state, the depolarization of the 3c-2e$^-$ bond, and the subsequent H_2 desorption—should provide important details into the efficiency of this process. It is clear from the measured cross sections (Figure 3C) that the desorption rates are comparable to those of typical photochemical processes occurring on idealized semiconducting oxides such as TiO_2.[32] Given our model for photochemically splitting the Ru_{cus}−H_2 bond, the key step in the chain of events above is likely the redistribution of charge in the $RuO_2(110)$ surface. This must be relatively long-lived in order for the depolarization process to desorb H_2 at the temperatures employed in this study (5−40 K). Otherwise, one would expect that rapid screening and de-excitation of the ES (both phenomena prevalent in metals) should significantly moderate any influence of the redistribution process on the polarization of the Ru_{cus}−H_2 complex. This, in itself, suggests that the $RuO_2(110)$ surfaces possess a degree of semiconductor-like character in its electronic structure despite the bulk being metallic. Therefore, the nonthermal properties of this cocatalyst should not be overlooked in obtaining a full understanding of its role in heterogeneous photocatalytic energy conversions.

■ ASSOCIATED CONTENT

Supporting Information

The Supporting Information is available free of charge on the ACS Publications website at DOI: 10.1021/jacs.6b05083.

Experimental and theoretical methods and data (PDF)

■ AUTHOR INFORMATION

Corresponding Authors

*ma.henderson@pnnl.gov

*roger.rousseau@pnnl.gov

Present Address

†Key Laboratory for Green Chemical Technology of Ministry of Education, School of Chemical Engineering and Technology, Tianjin University, Collaborative Innovation Center of Chemical Science and Engineering, Tianjin 300072, China

Notes

The authors declare no competing financial interest.

■ ACKNOWLEDGMENTS

This work was supported by the U.S. Department of Energy, Office of Science, Office of Basic Energy Sciences, Division of Chemical Sciences, Geosciences & Biosciences and performed in EMSL, a national scientific user facility sponsored by the Department of Energy's Office of Biological and Environmental Research and located at Pacific Northwest National Laboratory (PNNL). PNNL is a multiprogram national laboratory operated for DOE by Battelle.

■ REFERENCES

(1) Maeda, K.; Domen, K. *J. Phys. Chem. Lett.* **2010**, *1*, 2655.
(2) Maeda, K.; Takata, T.; Hara, M.; Saito, N.; Inoue, Y.; Kobayashi, H.; Domen, K. *J. Am. Chem. Soc.* **2005**, *127*, 8286.
(3) Maeda, K.; Teramura, K.; Lu, D. L.; Takata, T.; Saito, N.; Inoue, Y.; Domen, K. *Nature* **2006**, *440*, 295.
(4) Sato, J.; Saito, N.; Yamada, Y.; Maeda, K.; Takata, T.; Kondo, J. N.; Hara, M.; Kobayashi, H.; Domen, K.; Inoue, Y. *J. Am. Chem. Soc.* **2005**, *127*, 4150.
(5) Maeda, K.; Teramura, K.; Masuda, H.; Takata, T.; Saito, N.; Inoue, Y.; Domen, K. *J. Phys. Chem. B* **2006**, *110*, 13107.
(6) Over, H. *Chem. Rev.* **2012**, *112*, 3356.
(7) Weaver, J. F. *Chem. Rev.* **2013**, *113*, 4164.
(8) Qu, J. P.; Zhang, X. G.; Wang, Y. G.; Xie, C. X. *Electrochim. Acta* **2005**, *50*, 3576.
(9) Wang, J. H.; Fan, C. Y.; Sun, Q.; Reuter, K.; Jacobi, K.; Scheffler, M.; Ertl, G. *Angew. Chem., Int. Ed.* **2003**, *42*, 2151.
(10) Sun, Q.; Reuter, K.; Scheffler, M. *Phys. Rev. B* **2004**, *70*, 235402.
(11) Kubas, G. J. *Acc. Chem. Res.* **1988**, *21*, 120.
(12) Kubas, G. J.; Ryan, R. R.; Swanson, B. I.; Vergamini, P. J.; Wasserman, H. J. *J. Am. Chem. Soc.* **1984**, *106*, 451.
(13) Crabtree, R. H. *Angew. Chem., Int. Ed. Engl.* **1993**, *32*, 789.
(14) Heinekey, D. M.; Oldham, W. J. *Chem. Rev.* **1993**, *93*, 913.
(15) Kubas, G. J. *Chem. Rev.* **2007**, *107*, 4152.
(16) Jacobi, K.; Wang, Y.; Ertl, G. *J. Phys. Chem. B* **2006**, *110*, 6115.
(17) Crihan, D.; Knapp, M.; Seitsonen, A. P.; Over, H. *J. Phys. Chem. B* **2006**, *110*, 22947.
(18) Knapp, M.; Crihan, D.; Seitsonen, A. P.; Lundgren, E.; Resta, A.; Andersen, J. N.; Over, H. *J. Phys. Chem. C* **2007**, *111*, 5363.
(19) Wei, Y. Y.; Martinez, U.; Lammich, L.; Besenbacher, F.; Wendt, S. *Surf. Sci.* **2014**, *619*, L1.
(20) Jacobi, K.; Wang, Y.; Ertl, G. *J. Phys. Chem. B* **2006**, *110*, 22948.
(21) King, D. A.; Wells, M. G. *Surf. Sci.* **1972**, *29*, 454.
(22) Knapp, M.; Crihan, D.; Seitsonen, A. P.; Resta, A.; Lundgren, E.; Andersen, J. N.; Schmid, M.; Varga, P.; Over, H. *J. Phys. Chem. B* **2006**, *110*, 14007.
(23) Wei, Y. Y.; Martinez, U.; Lammich, L.; Besenbacher, F.; Wendt, S. *J. Phys. Chem. C* **2014**, *118*, 27989.
(24) Mu, R. T.; Cantu, D. C.; Glezakou, V. A.; Lyubinetsky, I.; Rousseau, R.; Dohnálek, Z. *J. Phys. Chem. C* **2015**, *119*, 23552.
(25) Mu, R. T.; Cantu, D. C.; Lin, X.; Glezakou, V. A.; Wang, Z. T.; Lyubinetsky, I.; Rousseau, R.; Dohnálek, Z. *J. Phys. Chem. Lett.* **2014**, *5*, 3445.
(26) Tait, S. L.; Dohnálek, Z.; Campbell, C. T.; Kay, B. D. *J. Chem. Phys.* **2005**, *122*, 164707.
(27) Over, H.; Seitsonen, A. P.; Lundgren, E.; Schmid, M.; Varga, P. *Surf. Sci.* **2002**, *515*, 143.
(28) Yang, Z. J.; Guo, Y. D.; Li, J.; Liu, J. C.; Dai, W.; Cheng, X. L.; Yang, X. D. *Chin. Phys. B* **2010**, *19*, 077102.
(29) de Almeida, J. S.; Ahuja, R. *Phys. Rev. B* **2006**, *73*, 165102.
(30) Goel, A. K.; Skorinko, G.; Pollak, F. H. *Phys. Rev. B* **1981**, *24*, 7342.
(31) Hakanoglu, C.; Hawkins, J. M.; Asthagiri, A.; Weaver, J. F. *J. Phys. Chem. C* **2010**, *114*, 11485.
(32) Henderson, M. A. *Surf. Sci. Rep.* **2011**, *66*, 185.

DOI: 10.1021/jacs.6b05083
J. Am. Chem. Soc. 2016, 138, 8714−8717